ARTICLE OPEN

Check for updates

Self-healable stretchable printed electronic cryogels for in-vivo plant monitoring

Eloïse Bihar[1]✉, Elliot J. Strand[2,6], Catherine A. Crichton[1,6], Megan N. Renny[2,6], Ignacy Bonter[3], Tai Tran[1], Madhur Atreya[1], Adrian Gestos[4], Jim Haseloff[3], Robert R. McLeod[2,5] and Gregory L. Whiting[1,2]✉

A key challenge in bioelectronics is to establish and improve the interface between electronic devices and living tissues, enabling a direct assessment of biological systems. Sensors integrated with plant tissue can provide valuable information about the plant itself as well as the surrounding environment, including air and soil quality. An obstacle in developing interfaces to plant tissue is mitigating the formation of fibrotic tissues, which can hinder continuous and accurate sensor operation over extended timeframes. Electronic systems that utilize suitable biocompatible materials alongside appropriate fabrication techniques to establish plant-electronic interfaces could provide for enhanced environmental understanding and ecosystem management capabilities. To meet these demands, this study introduces an approach for integrating printed electronic materials with biocompatible cryogels, resulting in stable implantable hydrogel-based bioelectronic devices capable of long-term operation within plant tissue. These inkjet-printed cryogels can be customized to provide various electronic functionalities, including electrodes and organic electrochemical transistors (OECTs), that exhibit high electrical conductivity for embedded conducting polymer traces (up to 350 S/cm), transconductance for OECTs in the mS range, a capacitance of up to 4.2 mF g^{-1} in suitable structures, high stretchability (up to 330% strain), and self-healing properties. The biocompatible functionalized cryogel-based electrodes and transistors were successfully implanted in plant tissue, and ionic activity in tomato plant stems was collected for over two months with minimal scar tissue formation, making these cryogel-based printed electronic devices excellent candidates for continuous, in-situ monitoring of plant and environmental status and health.

npj Flexible Electronics (2023)7:48 ; https://doi.org/10.1038/s41528-023-00280-1

INTRODUCTION

Significant technological advances over the past decade have enabled the development of electronics that can be integrated with living tissue using platforms such as e-skin[1], tattoo-like sensors[2], or implantable transient electronics[3] for treating, monitoring, or diagnosing health conditions. Recently, such devices have been explored for monitoring plant physiological parameters[4,5] which could be of significant utility to the agricultural industry, as well as for environmental monitoring. Devices such as organic electrochemical transistors (OECTs), organic ion pumps, and bioristors can be used to interface plant tissues with electronics and measure physiological changes within plant sap[5–8]. However, commonly used device substrates such as polyethylene terephthalate (PET), polyethylene naphthalate (PEN), or yarns can induce necrosis or death of plant tissues and limit long-term monitoring capabilities[8,9]. In these cases, patterning of the conducting traces and other required materials typically relies on fabrication techniques such as photolithography or approaches like blade coating that have limited patterning capability[10,11].

Soft electronics have potential application in various fields, including soft robotics, neuromorphic systems, biosensing, and others. As such there has been an emphasis on developing approaches that offer new pathways to the creation of these soft devices[12]. One promising avenue is the use of cryogels, which are a type of hydrogel formed through repetitive freeze-thaw cycling. These soft materials possess tuneable mechanical properties and are biocompatible. Cryogels have previously been used for tissue engineering and drug delivery, and present a high potential as 3D scaffolds for volumetric cell cultures[13]. Cryogels can have sponge-like macroporous structures with shape memory properties, and can be finely tuned to mimic the properties of biological tissues such as skin or plant matter (including stems and leaves)[14,15]. Among cryogel materials, polyvinyl alcohol (PVA) stands out as a cost-effective, biodegradable polymer that exhibits good mechanical, thermal, and biocompatibility properties, and has been used for decades to form cryogels and adhesives[14]. Physical crosslinking of PVA through cryogenic freeze-thaw cycling eliminates the need for potentially cytotoxic chemical crosslinkers or initiators, making them suitable for biomedical, particularly implantable, applications.

Previous studies have described methods to incorporate electroactive materials, including conducting polymers, like poly(3,4-ethylenedioxythiophene) polystyrene sulfonate (PEDOT:PSS), into hydrogels[15]. One of the main challenges in electronic gels is balancing conductivity and mechanical properties, as most conducting inks require high-temperature processes that are incompatible with hydrogels. PEDOT:PSS, being a biocompatible conducting polymer with excellent chemical stability and processability in aqueous solutions, is an ideal candidate for use in gel matrices. Researchers have developed self-adhesive conductive polymer composites by combining citric acid, cyclodextrin, PVA crosslinked with glutaraldehyde (GA), and PEDOT:PSS. These

[1]Paul M. Rady Department of Mechanical Engineering, University of Colorado Boulder, 1111 Engineering Drive, Boulder, CO 80309, USA. [2]Materials Science and Engineering, University of Colorado Boulder, 4001 Discovery Drive, Boulder, CO 80303, USA. [3]Department of Plant Sciences, University of Cambridge, Downing Street, Cambridge CB2 3EA, UK. [4]Materials Instrumentation and Multimodal Imaging Core Facility, University of Colorado Boulder, 1111 Engineering Drive Boulder, Boulder, CO 80309, USA. [5]Department of Electrical, Computer, and Energy Engineering, University of Colorado Boulder, 1111 Engineering Drive, Boulder, CO 80309, USA. [6]These authors contributed equally: Elliot J. Strand, Catherine A. Crichton, Megan N. Renny. ✉email: eloise.bihar@colorado.edu; gregory.whiting@colorado.edu

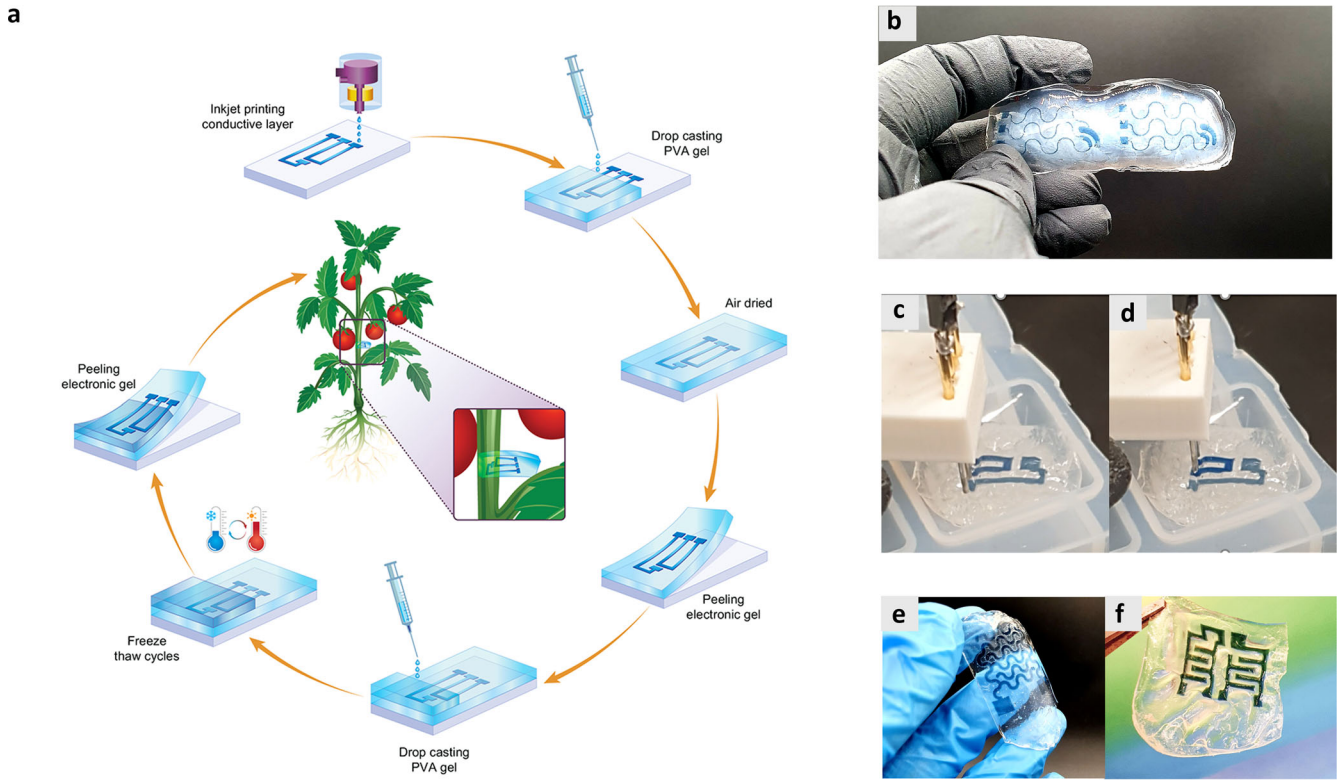

Fig. 1 Fabrication process of electronic gels. a Schematic of the fabrication steps of the electronic cryogels. First, the electronic trace is inkjet-printed on a glass slide. The first layer of hydrogel is then deposited on top of the conductive trace and is air-dried overnight, the gel is then peeled from the glass slide. Next, the second layer of wet hydrogel is drop-cast on top of the first air-dried layer of gel over the sensing area. Finally, the sample is placed in a freezer at −20 °C overnight. After a few freeze-thaw cycles, the electronic cryogel is ready for use, and placed inside a tomato plant stem. **b** Digital photographs of stretchable cryogel-based OECTs. **c**, **d** Photographs of the electrochromic properties of a PEDOT:PSS conducting layer in a transistor (OECT) configuration. **e** Photographs of a stretchable cryogel-based capacitor and **f** Cryogel-based electronic circuit comprising one OECT and two capacitors.

composites have been used to fabricate self-adhesive films for applications like electromyography, achieving high conductivity of up to 37 S cm^{-1}[15]. The rheological properties of PEDOT:PSS aqueous inks are compatible with low-cost printing processes, making it suitable for applications where printed flexible electronic devices are used, including for biomedical devices[16–18], as well as for agricultural use where collections of large numbers of devices are often needed to capture spatial variability[19]. Recent investigations have also explored the self-healing properties of conducting polymers, including the use of PEDOT:PSS in quasi-solid-state polymer electrolytes for OECTs[20]. In that study, the authors observed that the electrolyte contributed to the self-healing of the PEDOT:PSS film treated with Triton X-100 when used as a quasi-solid-state polymer electrolyte for organic electrochemical transistors (OECTs).

Directly interfacing electronic sensors with plant tissues could provide valuable insights about plant and ecosystem health. As such, OECTs and electrodes have been investigated for assessing plant status both in vivo and ex-vivo by monitoring various signals of interest[4,5,8,9,21–23]. For example, Luo, et al. used thermogels as morphable electrodes on leaves for plant electrophysiology[24], and Li, et al. developed an on-demand plant-based actuator using a poly(acrylic acid) hydrogel to create conformable electrodes used cutaneously with venus fly traps[25]. These approaches are typically limited to relatively short-term continuous in-vivo use as implants, since the substrates used can contribute to the formation of cork tissue[8]. Additionally, ensuring robustness towards the deformation and stresses triggered by plant growth poses a significant challenge in the long-term implantation of electronic devices into plant tissue[26].

In this study, we introduce an approach for implantable printed electronics by incorporating highly conducting inkjet-printed PEDOT:PSS traces into PVA cryogel matrices, thereby forming robust, biocompatible electronic cryogels that can sustain significant deformation and damage, and allow for long-term use inside plant tissue. To achieve this goal the electronic material (PEDOT:PSS) is first printed onto a glass slide, an initial layer of PVA hydrogel is then drop-cast onto the slide and is air-dried. Finally the completed device is peeled from the slide to give a freestanding (Fig. 1a) structure. The part of the device in contact with the biological fluid or tissue is then physically crosslinked through a cryogenic freeze-thaw method. These electronic cryogels provide useful properties such as significant tunability of the Young's modulus (in the kPa range), long-term stability in biological tissues (as demonstrated in tomato plant stems), ease of fabrication (using printing or casting approaches), robustness including mechanical stretchability (up to 330% strain), self-healing properties, and design flexibility. Here, inkjet printing is used to deposit the PEDOT:PSS traces, which is a versatile fabrication method that enables facile customization of the devices into various patterns. Different device functionalities have been evaluated, including OECTs (Fig. 1b–d), capacitors (Fig. 1e), and circuits (Fig. 1f). PEDOT:PSS traces incorporated into electronic cryogels also display high conductivity (up to 350 S cm^{-1}), and a high transconductance in vivo (mS range) in OECT structures. We successfully established and maintained communication inside a tomato plant stem for over two months using cryogel-based electronics with minimal hypersensitive tissue response, and monitored ion transport through impedance spectroscopy.

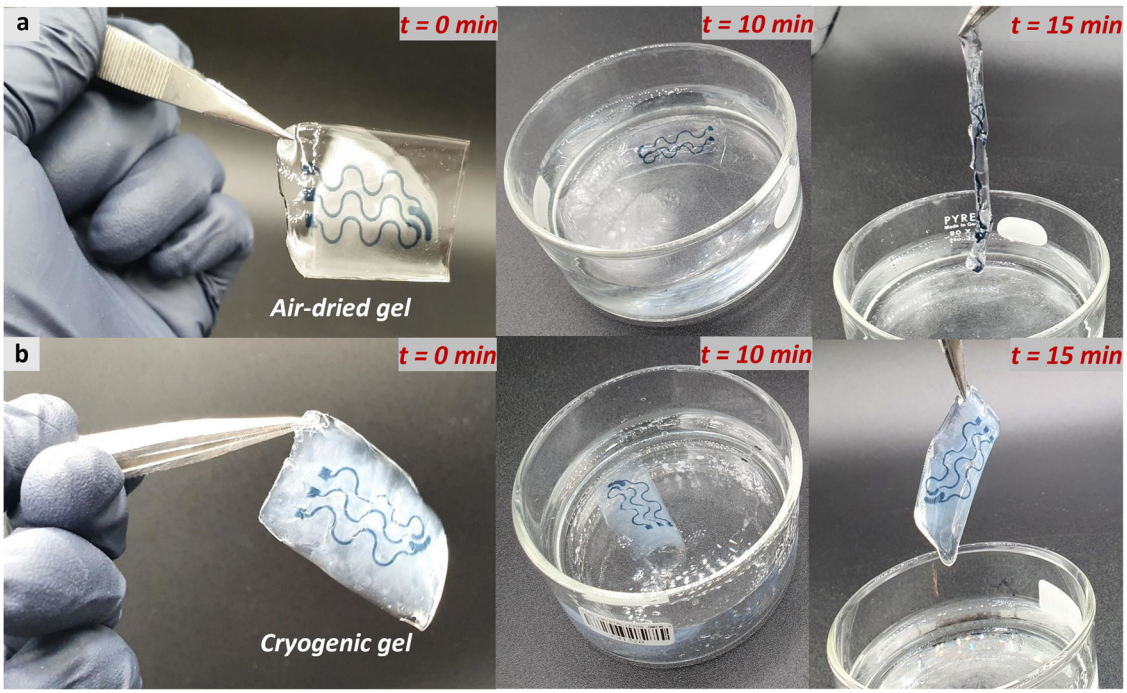

Fig. 2 Electronic gels: stability in media. a Air-dried electronic gels and **b** electronic cryogels. The air-dried electronic gel and cryogel are immersed in deionized water for 15 min and then the air-dried electronic gel and cryogel are extracted from the aqueous media.

RESULTS AND DISCUSSION

Fabrication and patterning of the electronic cryogels

Evaluating the performance of biomedical implants requires considering two sets of characteristics: biocompatibility and biofunctionality. Progress in the field of organic conducting materials has made satisfying electronic requirements and biocompatibility needs relatively straightforward[27]. Alloys and metals, however, are subject to corrosion, as such their use is a concern in the biological milieu. The nature of the substrate/matrix is also integral to the performance and stability of the device. Synthetic polymers such as silicon rubber, polyethylene (PE), parylene C, or polymethylmethacrylate (PMMA) are usually favored for soft and hard tissue applications[28–30]. Hydrogels are also useful due to their biocompatibility, ease of processing, and mechanical properties that can be tuned to mimic soft tissue. They can additionally be used as scaffolds for cell cultures and for drug delivery. PVA hydrogels are a promising material for medical devices due to their low protein adsorption characteristics, water solubility, and biocompatibility[31]. To create electronic traces on cryogels, we used a peeling method involving an inkjet-printed electronic feature made of the conducting polymer PEDOT:PSS with a drop-cast layer of PVA gel on top (Fig. 1a). The PEDOT:PSS electronic feature with drop-cast PVA was left to dry overnight and then peeled. Air-dried PVA gels, however, cannot be used directly as they are unstable due to high solubility in water (Fig. 2a). To make the gels insoluble in water, PVA needs to either be chemically or physically crosslinked. Here, we have addressed this issue by implementing the physical crosslinking method of cryogelation, which utilizes freeze-thaw cycling, and maintains the PVA's biocompatibility as it does not require the use of additional, potentially cytotoxic, chemical agents for crosslinking. In this study, electronic traces have been incorporated into a physically crosslinked PVA cryogenic gel. To stabilize the hydrogels a second layer of liquid PVA gel is drop-cast onto the peeled, air-dried PVA/PEDOT:PSS structure, which partially redissolves the underlying non-crosslinked PVA layer. Finally, the complete structure is physically crosslinked using a freeze-thaw (FT) cycling method to form a cryogel (Fig. 1a). The electronic cryogels (a composite of a cryogel and electronic materials) present improved structural stability in biological media (Fig. 2b) as they retain up to 97 +/−2 % of their original weight after 14 days implanted into living plant tissue (tomato plant stems), and maintain their electronic properties in aqueous media (Supplementary Fig. 1).

Mechanical and electrical performance of the electronic cryogels

Previous studies have shown that the mechanical properties of PVA hydrogels can be tailored by varying process parameters such as the concentration of the polymer, its chemical properties (molecular weight), and the gelation process[31,32]. Controlling hydrogels' mechanical properties enable their use in a wide range of medical devices[13,33]. Here, the mechanical properties of the different hydrogel compositions with varying molecular weights and processesing parameters were evaluated using tensile testing. Air-dried PVA hydrogels displayed a Young's modulus in the MPa range, but limited ductility as they only sustain up to around a 70% strain (Supplementary Fig. 2). Cryogels on the other hand can be stretched up to more than 300% strain before failure. The cryogels synthesized using a freeze-thawing method exhibited a highly porous sponge-like structure compared to the air-dried samples, (Supplementary Fig. 3) with pore size in the micrometer range which can be tuned by the experimental synthetic conditions[34]. Implementing a freeze-thaw method also increased the elongation ratio dramatically from 70% to up to 275%, and significantly decreased Young's modulus. As shown in Fig. 3a, formulated cryogels (composed of one layer of air-dried PVA followed by one layer of freeze-thawed gel) exhibited an elastic modulus of around 1.74 kPa. The cryogel elongation ratio was found to be dependent on the molecular weight of the PVA and its solution concentration. The mechanical properties of the cryogels can also be tuned by varying the freezing time as well as the number of freeze-thaw cycles (Supplementary Fig. 4). Similar to pure cryogels, increasing the molecular weight or the PVA percentage of the electronic cryogel increases the stretchability limits of the gel up to 330% strain (Supplementary Fig. 3b, c). Hence, combining both methods enables the mechanical

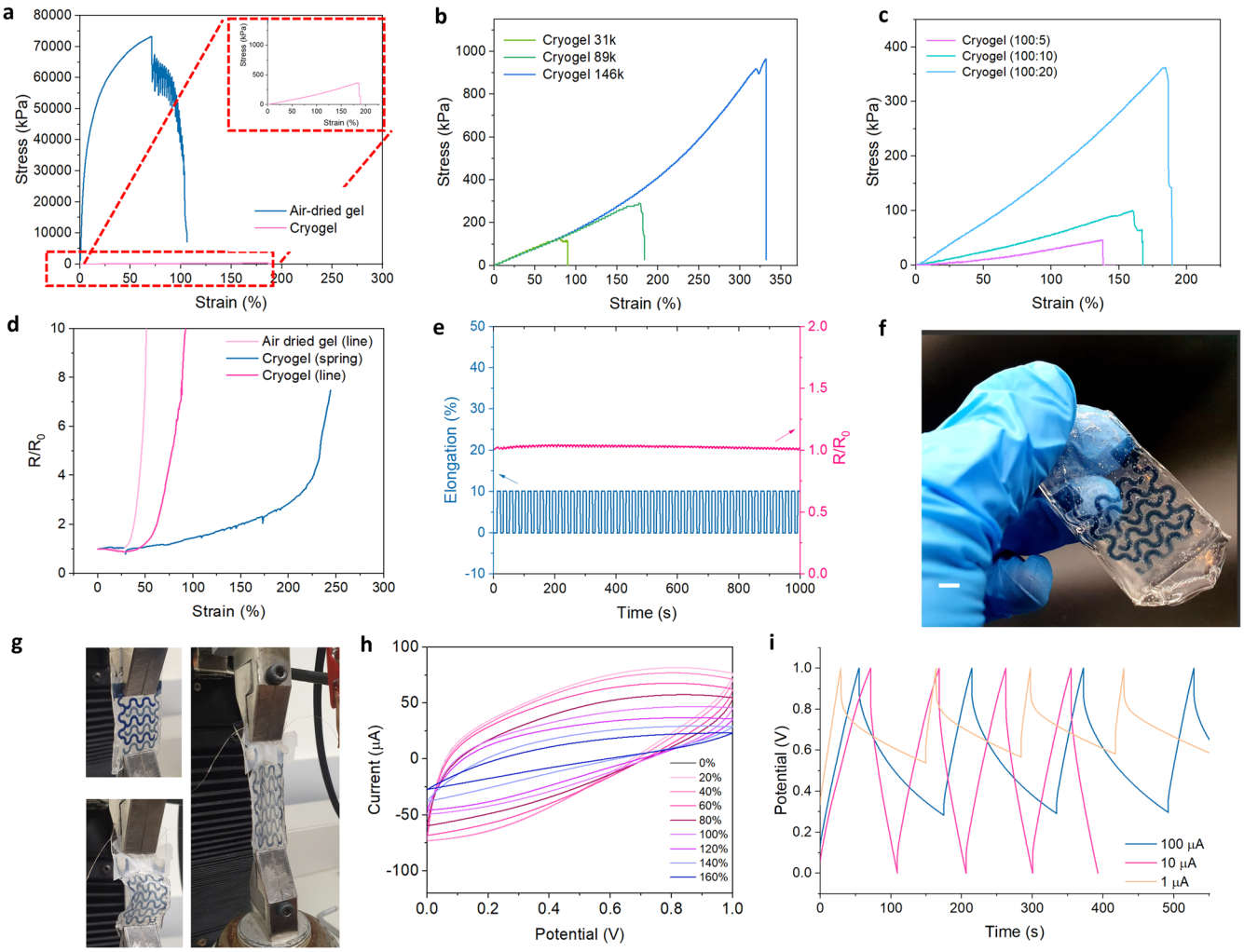

Fig. 3 Mechanical and electrical performance of electronic hydrogels. a Stress-strain curves for an air-dried gel and a cyrogel (0–300%). **b** Stress-strain curves (kPa) for cryogels with varying molecular weights and **c** PVA:H_2O compositions. **d**. Electrical resistance ratio for line-shaped PEDOT:PSS traces in an air-dried gel (printed lines (5×0.2 cm^2)) and in a cryogel, as well as a cryogel with serpentine PEDOT:PSS traces. **e** Electrical resistance ratio R/R_0 of an electronic cryogel for 100 cycles of 10% strain. **f** Photograph of a printed cryogel-based capacitor (Scale bar is 5 mm). **g** Photograph of a printed capacitor stretched while performing cyclic voltammetry **h** Cyclic voltammetry cycles within an applied voltage window range from 0 to 1 V for a printed capacitor under various strain conditons measured at a scan rate of 50 mV s^{-1}. **i** Galvanostatic charge/discharge curves of capacitor cryogels at varying current densities (1 μA, 10 μA, 100 μA) (the current density for charging is fixed at 100 μA) within an applied voltage range from 0 to 1 V.

properties to be extensively tuned (Young's modulus in the kPa range). The electronic properties of the hydrogels with PEDOT:PSS traces under different strains were also examined (Supplementary Fig. 5). As observed in Fig. 3d, the relative resistance (R/R_0) showed a more rapid change for the air-dried gel than for the cryogel. To further improve the electrical resistance of the sensor while under mechanical stress, we changed the electronic features from straight lines into wavy lines. Spring-shaped lines such as serpentine shapes or fractal-inspired features have been shown to withstand greater mechanical deformation/applied stress[3,35]. Modifying the geometry of the trace reduced the sensitivity of the trace to mechanical deformation (Fig. 3d). The cryogel with spring-shaped conductive features retains its electrical properties with an R/R_0 of 1.45 up to 100% strain, four times higher than the air-dried line-shaped trace, and twice that of the cryogel line-shaped structure. The cryogel spring-shaped trace is also mechanically and electrically stable when subject to repeated deformation under 10% cyclic stretching tests (Fig. 3e).

PVA hydrogels combined with ionically conductive species display high specific capacitance (in the mF cm^{-2} range) and were reported previously in the literature as solid-state supercapacitors when doped with acid as the conductive species[36]. Here, we have printed interdigitated capacitors (Fig. 3f) and performed cyclic voltammetry under different strains (Fig. 3g, h). These devices exhibit a planar capacitive sensing behavior with a specific capacitance of up to 4.2 mF g^{-1}. Increases in porosity/bulk ratio of the electrolyte improve the electrochemical performance of the capacitor under stress and help maintain its specific capacitance. The ionic properties of PEDOT:PSS favor the ion's penetration into the electrode bulk. The cryogel capacitor with spring-shaped electrode traces can be stretched up to 160% before failure and retains up to 60% of its initial specific capacitance at strains up to 100%. In comparison, solid-state spring-shaped capacitors only retain 30% of their initial specific capacitance at applied strains up to 60% (Supplementary Fig. 6a) confirming the stability of the device under mechanical deformation. The discharge characteristics for each current density (from 1 μA to 100 μA) are linear, further corroborating the capacitive behavior of the cell (Fig. 3i, Supplementary Fig. 6b).

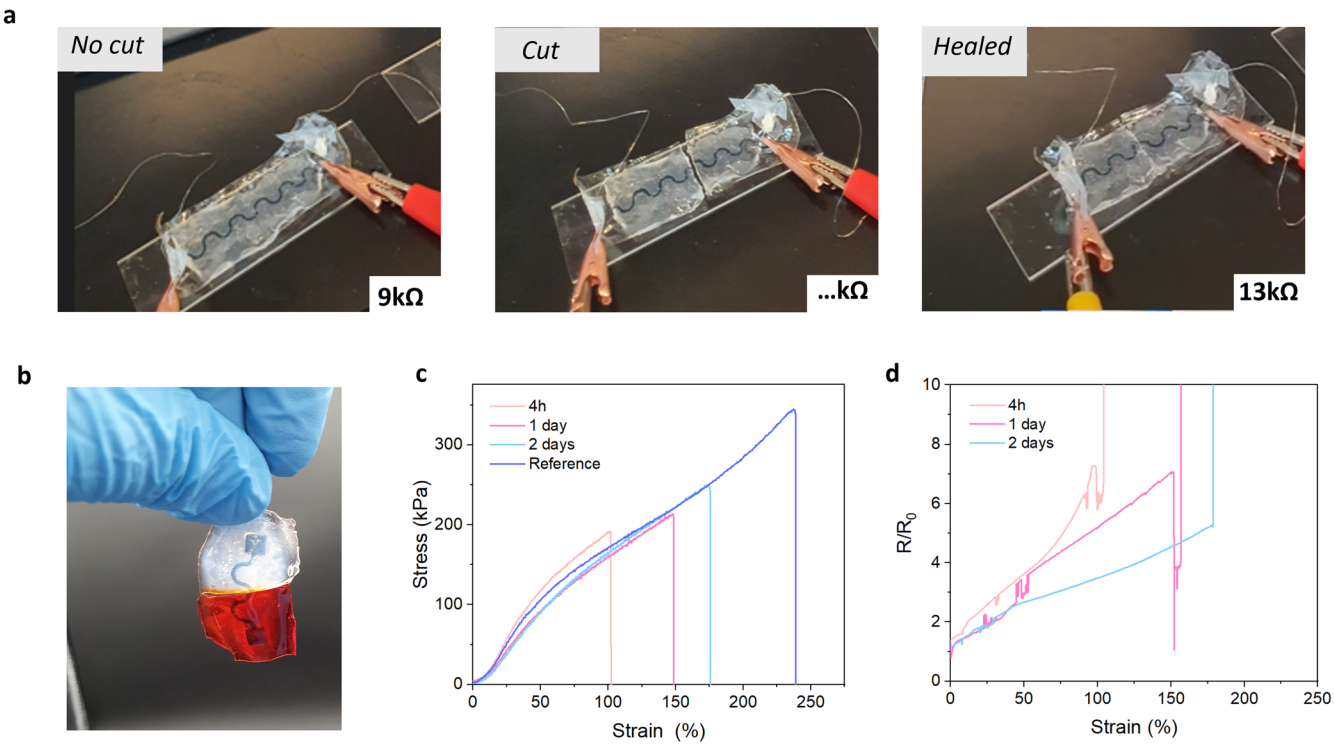

Fig. 4 Self-healing and recovery of electronic gels. a Image of a spring-shaped electronic cryogel (prepared with a freezing time of 30 min) connected to a source meter. The electrical resistance was originally 9 kΩ, the sample was then cut and separated, and placed back together. After 15 min, the electrical resistance of the sensor recovered to 13 kΩ. **b** Photograph of a self-healed cryogel **c** Stress-strain curves of uncut (reference) and cut electronic cryogels under taken after 4 h, 24 h, and 48 h healing time. **d**. Electrical resistance ratio of the spring-shaped electronic cryogel: uncut (reference) and cut under varying strain applied after 4 h, 24 h, 48 h of healing time.

Self-healing properties of the electronic gels

PVA-based hydrogels were also investigated for their self-healing capabilities which provide robustness and bring various opportunities for bioelectronic applications, particularly for electronic skins. Previous studies have demonstrated that hydrogels with a high concentration of PVA showed self-healing properties[37]. The freeze-thaw method produces stable, physically crosslinked hydrogels that can recreate physical interactions such as the hydrogen bonds at cut sites (Fig. 4a). Physical crosslinking of the hydrogel is attributed to the formation of crystalline regions at low temperatures. Self-repair capability depends on a plethora of parameters such as the molecular weight of the polymer or the gel composition, the number of freeze-thaw cycles, and the temperature. All these parameters influence the chain mobility of the polymer and its recovery after being cut. In this study, we prepared different compositions of PVA cryogels and evaluated their recovery after being cut through an investigation of their mechanical properties (Supplementary Fig. 7). Reducing the freezing time (from 2 h to 30 min) improved the self-healing capabilities as it decreased crosslinking between the chains. According to Zhang, et al.[37], the self-healing ability of a PVA cryogel is expected to depend on the formation of hydrogen bonds between PVA chains, and therefore is linked to the number of hydroxyl groups present. As such, increasing crosslinking density would be expected to reduce the possibility of recreating hydrogen bonding between PVA chains. Following repair, the mechanical properties of the healed samples were evaluated under stress (Supplementary Fig. 7a). Supplementary Fig. 7b shows stress-strain curves of the pure cryogels with different durations of healing. The pure cryogel samples were able to regain up to 155% strain after 48 h of healing at room temperature, which is 66% of the maximum elongation when compared with pristine samples. As also noted by Ko, et al.[31,38], we observed that the freeze-thaw duration of the PVA cryogel, hence the crosslinking density, plays an important role in the rearrangement of the PEDOT:PSS polymer chains and its healing after being damaged (or cut) (Supplementary Fig. 7c). Reconnecting the electronic cryogels after a cut was challenging as it required precise alignment (Fig. 4b). The thickness of the printed conducting layer was in the micron range while the substrate thickness was on the order of 175 µm. The resistance of the spring-shaped trace after cutting increased from 9 kΩ up to 13 kΩ (1.5 ratio) after 15 min of healing (Fig. 4a), which later decreased to 11 kΩ after 2 days of healing. These healed samples were also able to be stretched up to 175% before rupture (Fig. 4c) with an electrical resistance loss ratio of 5.3. (Fig. 4d).

Physiological monitoring of tomato plants

Creating soft electronic implants that can match the properties of biological tissues and remain stable in aqueous media is of tremendous importance. Gel-based implants have proven to be minimally invasive in biological tissues[30]. Amongst them, PVA hydrogels have excellent biocompatibility and are used in the medical field as membranes for contact lenses, for drug delivery, and for artificial organs[22,28]. Using a physical crosslinking method removes the need for additional chemical crosslinking agents that could potentially be toxic and/or induce an inflammatory response. While gels' benefits for biomedical applications have been widely reported, no study we are aware of has evaluated their benefits while used as implantable substrates in plants. Like animals, plants are subject to immune reactions regulated by (phyto)hormones in response to foreign bodies reinserted into their stems. Therefore, one of the key elements of successful implantation is minimizing the formation of necrotic tissues. To evaluate the biocompatibility of the devices in stems, two cryogels were implanted through longitudinal cuts in tomato plants during

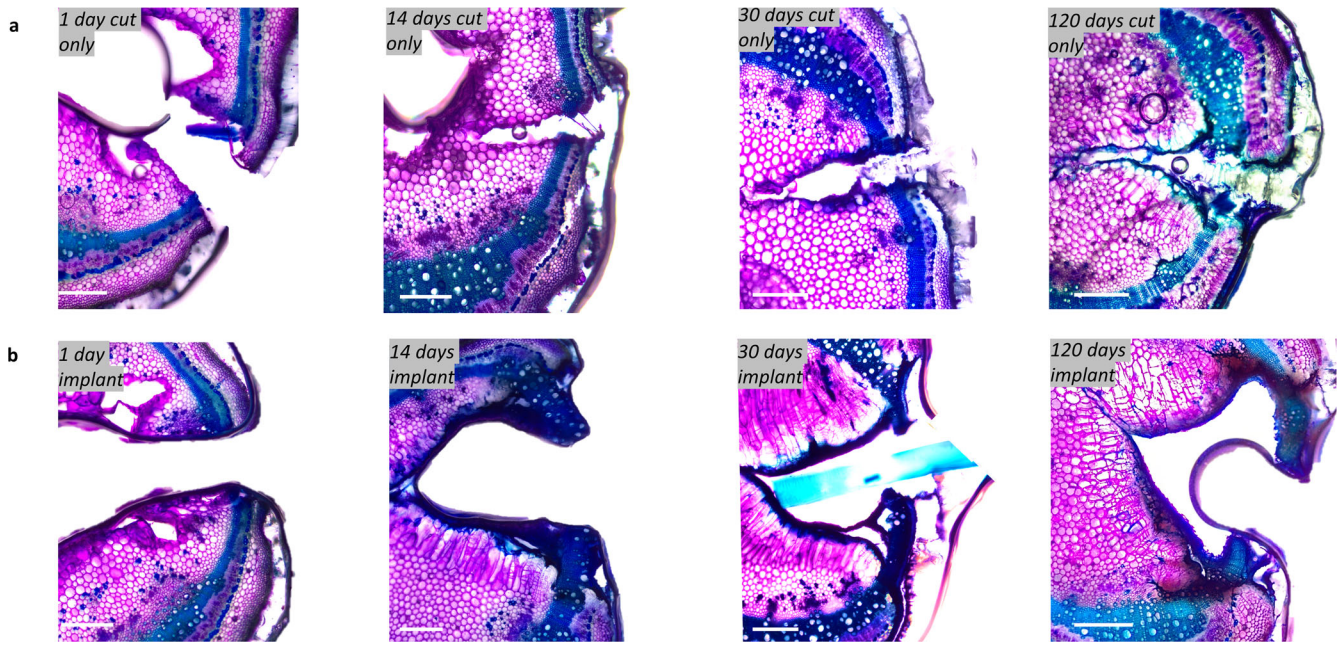

Fig. 5 Histology of tomato plant stems. Optical micrographs of transversal cuts of the tomato plant stem **a** without implants, and **b** with implants 1, 14, 30 and 120 days after implantation or cut (scale bar is 500 µm). In **b**, the implant is not always visible in the image as they were sometimes removed during the preparation process of the thin stem slices.

the growth phase, and cross sections of the stems (treated with toluidine blue o-based dye) were imaged via optical microscopy (Supplementary Fig. 8) over 120 days.

During the growth phase of the plant, the transport of ions through the stem takes place in the xylem and phloem. These vascular tissues, which convey nutrients between the roots and leaves, can be interrupted by immune responses to foreign bodies and the subsequent formation of necrotic tissues. We evaluated the formation of necrotic tissues and wound response around the tracheary elements of the stems. In both stems that had implants and simple cuts, we observed no lignification, which indicates no significant wound response 1 day after implantation (Fig. 5). After 2 weeks of implantation, we observed the formation of narrowed and elongated cells in the pith as a defense response, but a limited lignification of the tissues (Supplementary Fig. 9). In the xylem, the cells appear preserved while the epidermis and cortex cells retract over time. 30 days after implantation, the formation of a callus around the xylem at the wound interface was observed. The limited lignification of the tissue compared to the cut-only controls is also confirmed by X-ray computed tomography (Fig. 6a, b, and Supplementary Videos 1, 2). Analysis of the images confirms a reduced immune response after 1 week and 1 month of implantation as visible in the X-ray computed tomography data.

To further understand plant physiology and the movement of ions into sap, we evaluated xylem and phloem fluxes using impedance spectroscopy. Monitoring electrical signals in stems enables the detection of physiological changes due to hydration, nutritional uptake, and plant stress. Tomato plants in the growth phase have a high consumption of nutrients, especially potassium and nitrate ions[39]. Nutrient consumption can be evaluated through flow modulation on potassium uptake by roots. First, we assessed the stability of the printed cryogel in deionized water, as it will serve as the platform for monitoring plant health by measuring ionic fluxes in the vascular tissues. The impedance value of the electrodes does not vary significantly over 44 h. (+/− 2% of its original value after 44 h as shown in Supplementary Fig. 10). To evaluate nutrient uptake, two cryogel electrodes were surgically implanted into tomato plant stems (Fig. 7a). After implantation, the plant roots were first kept in tap water and after 7 days the growing fluid was replaced with a 300 mM solution of KCl. As shown in Fig. 7b, the impedance of the stem in water remains stable over time. On the other hand, when the plant roots become exposed to the KCl, we observe a decrease in the stem impedance over time due to the increase in K^+ concentration in the sap (Fig. 7c, Supplementary Fig. 11). It is worth pointing out the initial small increase in impedance (+ 9 kΩ at 995 Hz) in the first 10 min after KCl exposure could be attributed to transient water loss that reverses the bulk flow of the ionic solution in the xylem as previously reported for KCl treatments in tomato plants by Zakharin, et al.[40]. The measured impedance decreased significantly over 1 h as the plant takes up potassium ions.

Given this system of two electrodes across the plant tissue electrolyte, a Randles circuit consisting of a resistor in series with a resistor and capacitor in parallel describes the interaction between the printed PEDOT:PSS electrodes and the plant sap (electrolyte). In this scenario, the lone resistor can be considered the sum of contact and bulk solution resistance, R_s, the resistor in parallel with the capacitor can be considered as charge transfer resistance in the double layer, R_d, and the capacitor can be considered the double layer capacitance of the electrodes, C_d. However, since the substrate material consists of a permeable PVA hydrogel, there is likely ion diffusion through the gel, which further complicates the circuit model. The Nyquist plot (Fig. 7d) indicates two major changes in electrode response after transferring the tomato plant to KCl solution. After about 40 min of soaking in KCl solution, the resistance decreases. This can be interpreted as the electrodes experiencing an environment of higher salinity. Since PEDOT:PSS can undergo reversible oxidation-reduction reactions, the increase in cationic concentration would reduce the resistance associated with charge transfer (Faradaic) processes at the electrode surfaces. By Le Chatelier's principle, an increase in cations in the plant tissue would help reduce the energy required and the rate of reaction for this process. As a control experiment, the impedance signal was monitored when the stem was moved from a water container to a second water container. We compared the variation of the impedance at a fixed frequency, 995 Hz (Fig. 7e). The uptake of potassium ions in the tomato plant stem is noticeable after 60 min (−7.4 kΩ) compared to the control experiment (+1 kΩ) which is

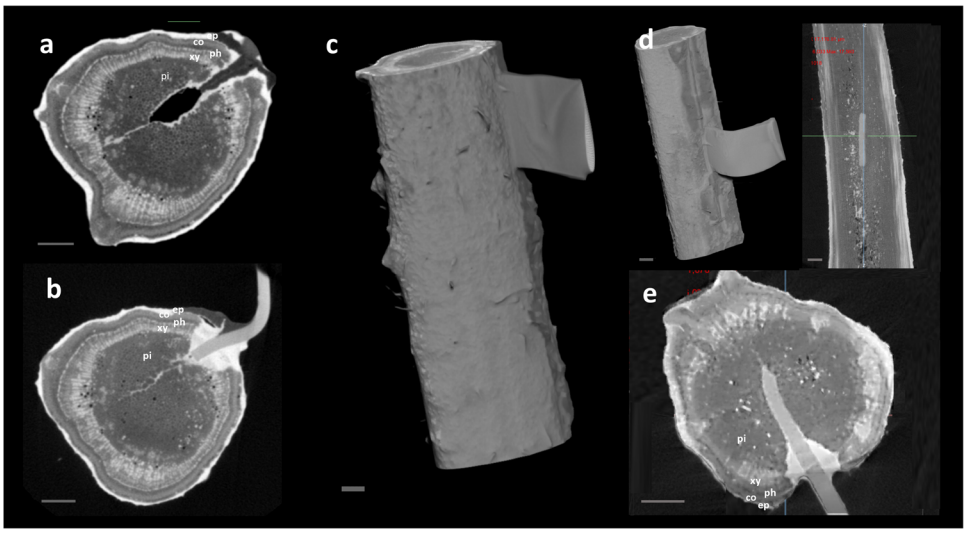

Fig. 6 X-ray computed tomography images. X-ray computed tomography images of the **a** cut-only, and **b** implants in tomato plant stems after 1 week. **c** X-ray computed tomography image of the implant after 1 week. **d** and **e** X-ray computed tomography images of implants in tomato plant stems after 1 month (scale bar is 1 mm) (ep: epidermis; co: cortex; ph: phloem tissue; xy: xylem tissue; pi: pith).

confirmed by the Nyquist plot. When the plant was repetitively exposed to solutions of KCl, indications of damage (potentially due to high potassium concentration) on day 25 after implantation were noticeable through the change in the modulation of the impedance signal (Supplementary Fig. 12).

We also investigated the impedance in tomato plant stems under drought conditions (Supplementary Fig. 13). Water was removed from the flask and the plant was left to dry for a duration of 24 h. The impedance values increased in drought conditions (Fig. 7f). Analysis of the circuit model and Nyquist plot, in Fig. 7g, suggest that under drought conditions R_s increases as the plant dries out (expanded with the overlaid model in Supplementary Fig. 14). This is unsurprising as plants with low water content also would have reduced ion mobility. Notably, R_d also increases, suggesting that there is also an additional barrier for ions to interact with the electrode surface. After 24 h in drought conditions, the variation in impedance reaches up to $+3140\,k\Omega$ at 995 Hz, while for the control experiments (the stem which remains in water, the impedance signal only shifts $+/-$ 5 kΩ over 15 days (Fig. 7h, Supplementary Figs. 15, 16). Repeating the experiment with different plants, we observed that the modulation of the impedance is influenced by the drying kinetics of the plant. (Supplementary Fig. 17).

In addition to impedance spectroscopy, organic electrochemical transistors (OECTs) are an interesting platform for interfacing biological signals with electronics as they use an electrolyte as an active component of the device. OECTs have a high transconductance and enable the amplification of biological signals. One of the advantages of cryogel OECTs is the ability to monitor in real-time the concentration of ions in the sap and the xylem transport rate by monitoring the drain current. We first compared the characteristics of air-dried and cryogel OECTs using a methylcellulose-based ionic gel as the electrolyte (Supplementary Fig. 18). The limit of detection (LOD) for the cryogel OECTs was estimated at around 50 μM for potassium ions (Supplementary Fig. 19). While the transconductance of the air-dried OECT is higher, crosslinking the gel is essential for providing stability when the device is in contact with the biological milieu. After being implanted in a tomato plant stem, a cryogel OECT exhibited a maximum transconductance of 1.41 mS on day 1 after implantation. In that configuration, the sap played the role of the electrolyte. The transconductance of the implant in the stem was recorded over 82 days (Supplementary Fig. 20).

The maximum transconductance of the cryogel OECT in the tomato plant stem 62 days after implantation was 1.17 mS, 82% of the original maximum transconductance value measured on day 1 (Fig. 8a, b). The variation of transconductance is attributed to the presence of lignified tissue which becomes more evident 120 days after implantation. To study the plants' vascular systems, we placed channel implants in healthy stems at different distances from the gate (5.7 cm, 9.5 cm, and 15 cm, respectively) (Fig. 8c) and measured drain current responses to different applied stimuli (gate pulses) (Supplementary Fig. 21). As expected, the further the channel is from the gate (up to 15 cm), the lower the transconductance of the device after applying a 1 min gate pulse. 7 days after implantation, the root system of the plant was submerged in 300 mM KCl and the time response of an OECT ($d_{channel\text{-}gate} = 5.7$ cm) to KCl stress was evaluated. The drain and gate currents within the stem were recorded over 9 h while 60 s gate pulses were repetitively applied (Fig. 8d). As shown Fig. 8e, the correspondence of the drain current with the uptake of ions by the plant and the variation of the drain current matches the change in impedance reported previously. Using an OECT configuration enables monitoring of the movement of ions through the stem in real-time (Fig. 8f), and demonstrates the delay in the biological stress and subsequent recovery response of the plant.

This study introduces a method for integrating highly conducting PEDOT:PSS traces into biocompatible PVA cryogel matrices, enabling the development of stable, implantable hydrogel-based bioelectronic devices for continuous, in-situ monitoring of plant and environmental status and health. These cryogels offer added benefits over other hydrogel-based approaches, including providing long-term stability inside plant tissue without the need for small molecule cross-linkers, photosensitizers, and other materials that may impact plant function. One of the challenges of implanting electronic devices into plant tissue is to maintain good resilience to deformation and stresses induced by plant growth. The electronic cryogels presented here are tuned to provide both self-healing properties and high stretchability, which are of significant importance for withstanding mechanical stress caused by plant growth and motion. We demonstrate that the cryogels' mechanical properties, such as stiffness and ductility, can be tailored through materials selection and synthetic process to match those of living tissues. The soft cryogels prevent the formation of lignified tissues

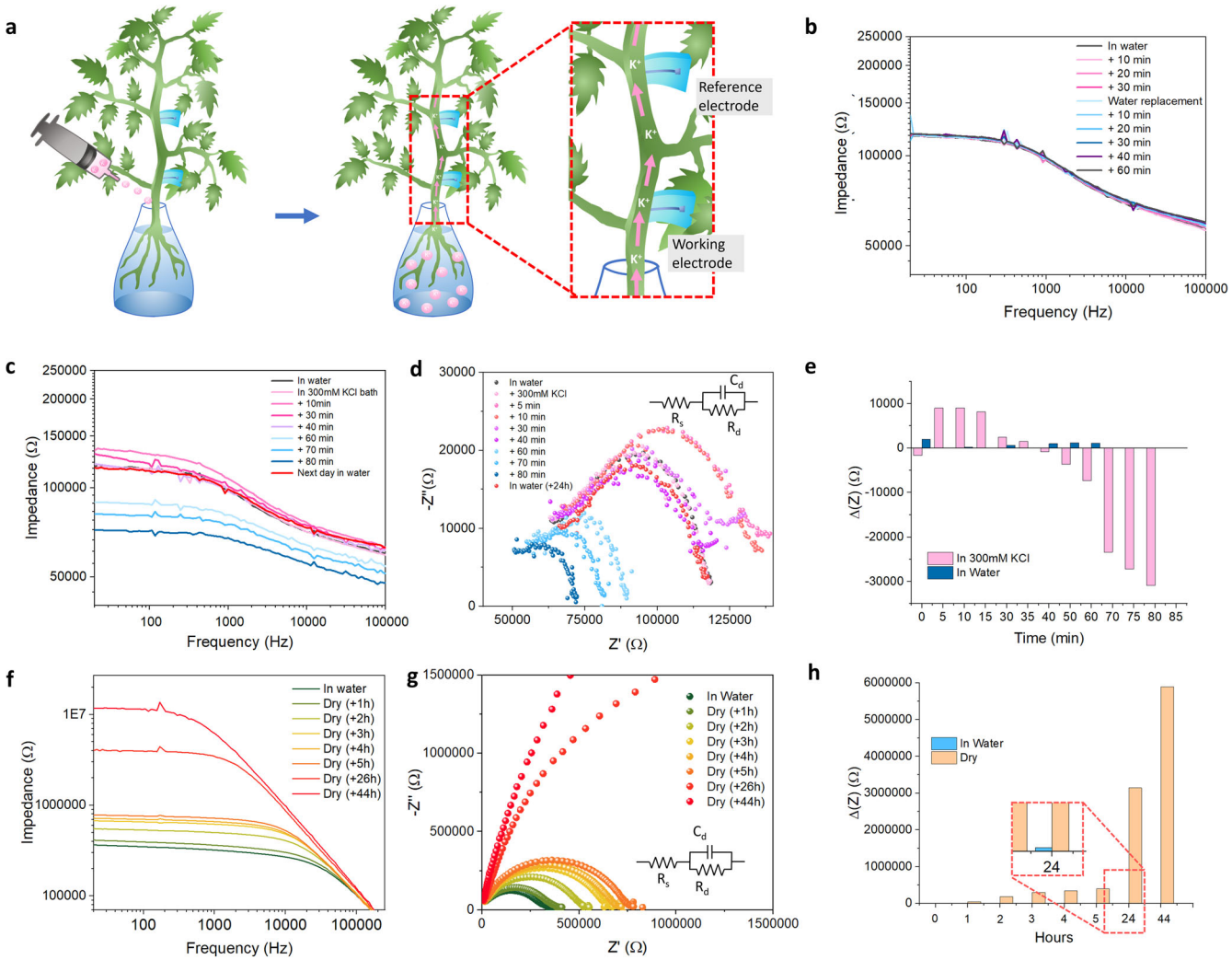

Fig. 7 Characterization of gel-based electrodes implanted in tomato plant stems. a Schematic showing cryogel electrodes implanted in a tomato plant stem before and after adding nutrients to the aqueous growing solution. Electrochemical impedance spectra were obtained from cryogel electrodes implanted in a tomato plant stem. Impedance was measured on day 7 after cryogel electrode implantation. The signals are recorded at different frequencies after transferring the plant from **b** a first water bath into a second water bath, and **c** from a water bath to an aqueous 300 mM KCl solution. **d** Nyquist plot of cryogel electrodes implanted in the stem and the plant roots immersed in an aqueous 300 mM solution KCl solution. **e** Comparison of the electrochemical impedance recorded from implants in a stem with the plant roots in water, and in an aqueous 300 mM KCl solution. **f** Electrochemical impedance spectra obtained from cryogel electrodes implanted in a stem with the plant experiencing drought conditions for 44 h (roots kept dry). For the control plant the roots were continuously submerged in water). The impedances are measured on day 14 after implantation. **g** Nyquist plot taken using the cryogel electrodes implanted in a stem and the plant removed from water and left for 44 h to dry. **h** Comparison of the electrochemical impedance taken using the cryogel electrodes between a tomato plant in water and a tomato plant left to dry for 44 h.

for long-term monitoring of plants and provides a matrix for electronics that elicits a limited cellular tissue immune response. As such, these printed electronic cryogel implants provide an effective platform for monitoring plant health inside of vascular tissues. Using soft hydrogel electronic implants enables a reliable and robust interface between electronics and vascular tissues for the measurement of sap contents over two months. This study demonstrates that the cryogel-based electrodes can track in vivo real-time response to different environmental situations, including water stress conditons, and changes in ion concentrations which could ultimately help to predict plant and growing media status and health. The useful properties of these cryogel-based devices, including high electrical conductivity, stretchability, self-healing capabilities, and long-term stability, make them promising candidates for applications in precision farming, environmental monitoring, and beyond.

METHODS

Materials and ink formulation

PEDOT:PSS: Clevios™ F.H.C. ink was purchased from Heraeus. PEDOT FHC was mixed with 1 wt.% of glycidoxypropyltrimethoxysilane (GOPS, Sigma Aldrich) to crosslink the PEDOT:PSS conductive trace[41]. The PEDOT:PSS ink concentration was 1–1.5% and its viscosity was 8–70 mPa s before the addition of the GOPS. The PEDOT:PSS inks were sonicated in an ultrasonic bath for 30 min and filtered using a 1.2 µm PTFE filter. For capacitors, PVA (Sigma Aldrich), H_3PO_4 (Sigma Aldrich), and deionized water were used.

Fabrication of the electronic cryogel

A Dimatix DMP-2800 desktop inkjet printer was used for the deposition of each layer with a 15 µm drop spacing. For the OECT, capacitor, and printed lines three layers of PEDOT:PSS were

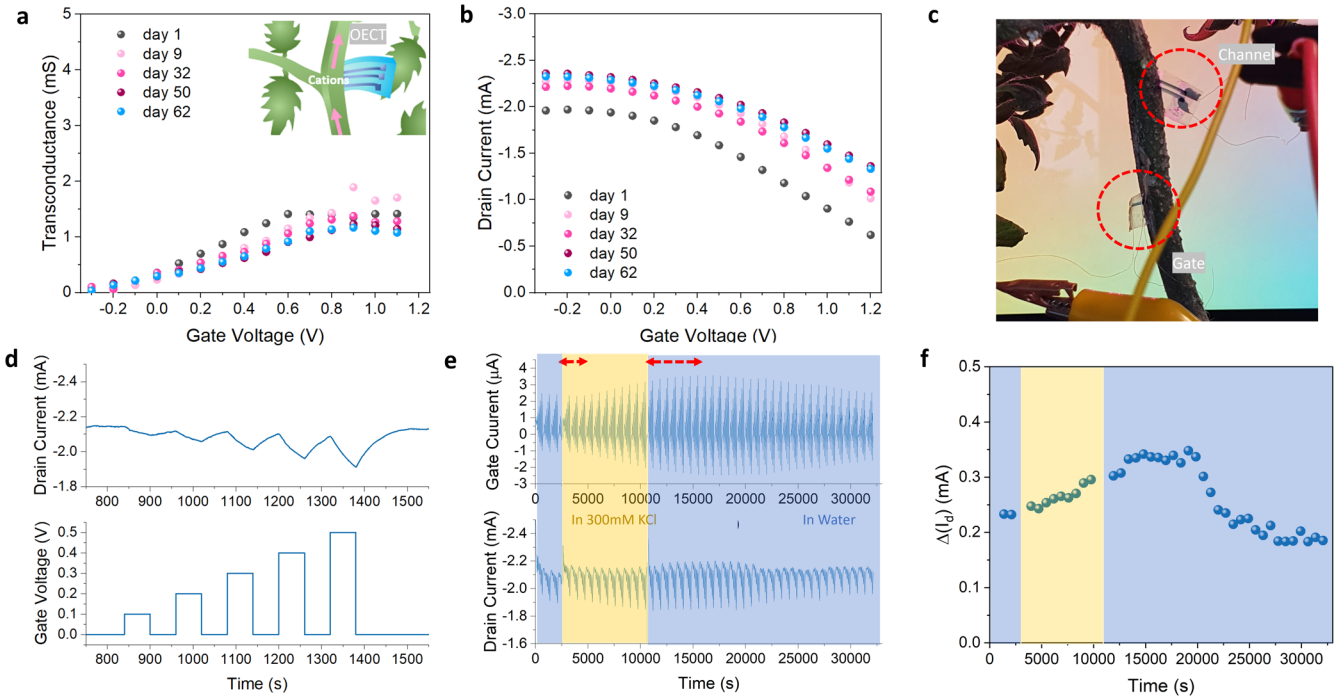

Fig. 8 Characterization of cryogel-based OECTs implanted into tomato plant stems. a Transconductance curve and **b** transfer curve of an OECT implant in a tomato plant stem over a period of 2 months. **c** Photograph of two cryogel implants in a tomato plant stem. The top implant is the gate, and the bottom implant is the channel **d** Drain currents for cryogel sensors in a tomato plant stem in response to applied gate pulses (0 V, 0.1 V, 0.2 V, 0.3 V, 0.4 V, and 0.5 V sequentially) in water 7 days after implantation. One cycle is 60 s on and 60 s off. **e** Gate and drain currents in response to gate pulses applied when the tomato plant roots are immersed in (day 7 after implantation) water (blue areas) and in KCl solution (yellow area). **f** Variation of the drain current at 0.5 V gate bias when the tomato plant roots are immersed in water (blue areas) and in KCl solution (yellow area).

printed on a glass substrate, wet on wet[42]. The printer plate temperature was kept at 50 °C and the ink at 30 °C. After printing, the conducting traces were dried on a hot plate at 90 °C under ambient conditions for 10 min. PVA-based gels were prepared by dissolving PVA in deionized water at various water:PVA weight ratios (100:5, 100:10, 100:20). Varying molecular weights of PVA were used (M_w 31,000–50,000 g mol^{-1}, 89,000–98,000 g mol^{-1}, 146,000–186,000 g mol^{-1}). The powder was dissolved in deionized water at 90 °C using magnetic stirring.

For the electronic cryogels for the implants after curing the conducting electrode, the first layer of gel electrolyte (deionized water:PVA weight ratio 100:10, and M_w 89,000–98,000 g mol^{-1}) was deposited, and was dried for 6 h at room temperature. Then, the device was peeled, and the second layer of electrolyte (deionized water:PVA weight ratio 100:20, and M_w 89,000–98,000 g mol^{-1}) was deposited on the area of interest and left to dry for 12 h in a freezer at −20 °C. Afterwards, a second freeze-thaw cycle was performed to finalize the cryogelation process.

Characterization of the electronic gels

Capacitor characterization. Chronopotentiometry measurements were carried out using a SP-150 Potentiostat-BioLogic. The specific capacitance C was deduced from the relation: $C_s = \frac{IdV}{Vm\Delta V}$ where C_s is in F g^{-1}, m is the mass in g, IdV is the integrated area under the CV curve, ΔV is the difference in the potential window, and V is the potential scan rate (mV s^{-1}). Cyclic voltammetry was carried out using an Emstat3 Blue potentiostat (Palmsens). The potential applied for cyclic voltammetry measurements was between 0 V and 1 V and the potential scan rate was 20 mV s^{-1}.

Mechanical characterization of the gels. An MTS Insight 2 electromechanical testing machine was used to perform the mechanical characterization (stretchability, cycles) of the electronic gel-based devices. A 2 kN cell load was used for the stretching experiments. For the failure tests, the load speed was 30 mm min^{-1}. For the mechanical testing, the dimensions of the cryogels and air-dried hydrogels were (L × W × T) 5.75 × 0.127 × 0.3175 cm^3 and 5.75 × 0.127 × 0.0175 cm^3, respectively. Viscosities of the gels used for the implants (with respective deionized water:PVA weight ratios (100:10, 100:20) were measured using an MCR 702e rheometer (Anton Paar) (see Supplementary Fig. 22).

OECT electrical characterization. The dimensions of the devices were: for the electrode/gate 2.5 × 2.5 mm^2, and for the channel 2 × 1 mm^2. The thickness of the air-dried gels was 0.175 +/− 25 mm, and 0.3 +/− 0.05 mm for the cryogels. A Keithley 2600 source-measure unit was used to characterize the OECT. For the characterization of the transistor, V_g varies from 0 V to 1.2 V, and V_d from −1.2 V to 0 V. For the chronoamperometric measurements, we applied a 30 s pulse while varying V_g from 0 V to 0.5 V and holding V_d at −0.8 V. Thin silver wires were glued to the OECT contacts for connection and left to dry overnight before use (Supplementary Fig. 23). The dimensions of the OECTs implanted in tomato plant stems were 2.5 × 2.5 mm^2 for the gate and 2 × 1 mm^2 for the channel. The thickness for the implants was 300 +/− 50 μm.

Self-healing tests. Two pieces of cryogel were prepared. The samples were stored for preparation in the freezer for a duration of 1–24 h. One piece was stained with food coloring to facilitate observation of the recovery of the gels after being cut. A razor blade was used to cut the devices into two halves, and they were placed back in contact and held in place for less than 10 s.

Microscopy. A SEMTT (Hitachi TM4000Plus II Tabletop SEM, W-filament system with Oxford EDS) was used for the acquisition of the SEM images of the electronic gels.

Plant growth

Red cherry tomato plants (Solanum Lycopersicum) were grown in hydroponic systems (Idoo) in a temperature-controlled environment with 24-Watt LED grow lights under a 16 h:8 h light-dark cycle. A diluted standard commercial hydroponic liquid fertilizer (EZ-gro Liquid Plant Food for Aerogardens) was used to feed the plants once per week during the growth phase. After implantation for the nutrient uptake experiment, the plants were left in tap water for 7 days. The experiments were carried out in a controlled environment where the humidity and the temperature were kept constant (21 °C, 30–50% relative humidity). To assess the effect of the implants on plant growth, we measured the levels of chlorophyll content and nitrogen concentration optically using a commercial meter (AMTAST), and observed that the implanted sensor did not appear to interfere with the normal growth or physiological status of the host plants (Supplementary Fig. 24).

Morphological characterization of the plants

The tomato plant stems were hand-sectioned using a razor blade and then were stained for 30 s using a dilute solution containing toluidine blue (0.01 wt.%). They were then placed in a 10% ethanol solution for 30 s and kept in deionized water. An Olympus microscope with an integrated Swift camera was used for the acquisition of the stitched images of the stem slices. The X-ray computed tomography images were taken using a ZEISS Xradia 520 Versa X-ray Microscope at 60 kV, 5 W, no filter, 0.4X objective, 1201 projections, binning of 2, 70 mm source to center distance and −30 mm detector to center distance. After 1 week and 1 month since implantation, respectively, the stems were cut and placed in a 10 wt% solution of cesium iodide for 15 h before imaging. During this study, 20 tomato stems were implanted with the gel sensors and tested and characterized for a duration of up to 81 days.

Impedance spectroscopy

Impedance spectroscopy was performed using an EmStat Pico (Palmsens) impedance analyzer over a frequency range of 22 Hz to 200 kHz. We applied a low potential (100 mV) to prevent interfering electrochemical reactions. To avoid the effect of the stress induced by implantation of the gel electrodes we waited 7 days minimum after implantation prior to collecting data.

DATA AVAILABILITY

The data that supports the figures and other findings of this study can be found at https://osf.io/8gzpn/ (https://doi.org/10.17605/OSF.IO/8GZPN)[43]. Additional information will also be provided by the authors upon reasonable request.

Received: 29 March 2023; Accepted: 6 October 2023;
Published online: 23 October 2023

REFERENCES

1. Baumgartner, M. et al. Resilient yet entirely degradable gelatin-based biogels for soft robots and electronics. *Nat. Mater.* **19**, 1102–1109 (2020).
2. Wang, Y. et al. Low-cost, μm-thick, tape-free electronic tattoo sensors with minimized motion and sweat artifacts. *Npj Flex. Electron.* **2**, 1–7 (2018).
3. Hwang, S.-W. et al. A Physically Transient Form of Silicon Electronics. *Science* **337**, 1640–1644 (2012).
4. Stavrinidou, E. et al. Electronic plants. *Sci. Adv.* **1**, e1501136 (2015).
5. Li, W. et al. An on-demand plant-based actuator created using conformable electrodes. *Nat. Electron.* **4**, 134–142 (2021).
6. Janni, M. et al. In Vivo Phenotyping for the Early Detection of Drought Stress in Tomato. *Plant Phenom.* **2019**, 1–10 (2019).
7. Roper, J. M., Garcia, J. F. & Tsutsui, H. Emerging Technologies for Monitoring Plant Health in Vivo. *ACS Omega* **6**, 5101–5107 (2021).
8. Diacci, C. et al. Diurnal in vivo xylem sap glucose and sucrose monitoring using implantable organic electrochemical transistor sensors. *iScience* **24**, 101966 (2021).
9. Coppedè, N. et al. An in vivo biosensing, biomimetic electrochemical transistor with applications in plant science and precision farming. *Sci. Rep.* **7**, 16195 (2017).
10. Irimia-Vladu, M., Glowacki, E. D., Sariciftci, N. S. & Bauer, S. *Green Materials for Electronics*. (John Wiley & Sons, 2017).
11. Song, J. & Yan, F. Applications of Organic Electrochemical Transistors in Flexible Bioelectronics. *IEEE J. Flex. Electron.* **1**, 88–97 (2022).
12. Liang, Q. et al. Highly Stretchable Hydrogels as Wearable and Implantable Sensors for Recording Physiological and Brain Neural Signals. *Adv. Sci.* **9**, 2201059 (2022).
13. Villard, P. et al. Autoclavable and Injectable Cryogels for Biomedical Applications. *Adv. Healthc. Mater.* **8**, 1900679 (2019).
14. Deng, J. et al. Electrical bioadhesive interface for bioelectronics. *Nat. Mater.* **20**, 229–236 (2021).
15. Tan, P. et al. Solution-processable, soft, self-adhesive, and conductive polymer composites for soft electronics. *Nat. Commun.* **13**, 358 (2022).
16. Bihar, E. et al. A fully inkjet-printed disposable glucose sensor on paper. *Npj Flex. Electron.* **2**, 1–8 (2018).
17. Li, L. et al. All Inkjet-Printed Amperometric Multiplexed Biosensors Based on Nanostructured Conductive Hydrogel Electrodes. *Nano Lett.* **18**, 3322–3327 (2018).
18. D. Garma, L., M. Ferrari, L., Scognamiglio, P., Greco, F. & Santoro, F. Inkjet-printed PEDOT:PSS multi-electrode arrays for low-cost in vitro electrophysiology. *Lab. Chip* **19**, 3776–3786 (2019).
19. Love, C. et al. A Review on Advanced Sensing Materials for Agricultural Gas. *Sens. Sens.* **21**, 3423 (2021).
20. Ko, J., Wu, X., Surendran, A., Muhammad, B. T. & Leong, W. L. Self-Healable Organic Electrochemical Transistor with High Transconductance, Fast Response, and Long-Term Stability. *ACS Appl. Mater. Interfaces* **12**, 33979–33988 (2020).
21. Burtscher, B., Leising, G. & Greco, F. Temporary Tattoo Approach for a Transferable Printed Organic Photodiode. *ACS Appl. Electron. Mater.* **3**, 2652–2660 (2021).
22. Gentile, F. et al. A Biomimetic, Biocompatible OECT Sensor for the Real-Time Measurement of Concentration and Saturation of Ions in Plant Sap. *Adv. Electron. Mater.* **8**, 2200092 (2022).
23. Armada-Moreira, A. et al. Benchmarking organic electrochemical transistors for plant electrophysiology. *Front. Plant Sci.* **13**, 916120 (2022).
24. Luo, Y. et al. A Morphable Ionic Electrode Based on Thermogel for Non-Invasive Hairy Plant Electrophysiology. *Adv. Mater.* **33**, 2007848 (2021).
25. Koman, V. B. et al. Persistent drought monitoring using a microfluidic-printed electro-mechanical sensor of stomata in planta. *Lab. Chip* **17**, 4015–4024 (2017).
26. Dufil, G., Bernacka-Wojcik, I., Armada-Moreira, A. & Stavrinidou, E. Plant Bioelectronics and Biohybrids: The Growing Contribution of Organic Electronic and Carbon-Based Materials. *Chem. Rev.* **122**, 4847–4883 (2022).
27. Balint, R., Cassidy, N. J. & Cartmell, S. H. Conductive polymers: towards a smart biomaterial for tissue engineering. *Acta Biomater.* **10**, 2341–2353 (2014).
28. Winslow, B. D., Christensen, M. B., Yang, W.-K., Solzbacher, F. & Tresco, P. A. A comparison of the tissue response to chronically implanted Parylene-C-coated and uncoated planar silicon microelectrode arrays in rat cortex. *Biomaterials* **31**, 9163–9172 (2010).
29. Kretlow, J. D. et al. Evaluation of Soft Tissue Coverage over Porous Polymethylmethacrylate Space Maintainers Within Nonhealing Alveolar Bone Defects. *Tissue Eng. Part C. Methods* **16**, 1427–1438 (2010).
30. França, D. C. C., de Castro, A. L., Soubhia, A. M. P., de Aguiar, S. M. H. C. Á. & Goiato, M. C. Evaluation of the Biocompatibility of Silicone Gel Implants – Histomorphometric Study. *Acta Inform. Med.* **21**, 93–97 (2013).
31. Baker, M. I., Walsh, S. P., Schwartz, Z. & Boyan, B. D. A review of polyvinyl alcohol and its uses in cartilage and orthopedic applications. *J. Biomed. Mater. Res. B Appl. Biomater.* **100B**, 1451–1457 (2012).
32. Fu, Z. et al. Hydrogen-bond-dominated mechanical stretchability in PVA films: from phenomenological to numerical insights. *Phys. Chem. Chem. Phys.* **24**, 1885–1895 (2022).
33. Bakhshpour, M., Idil, N., Perçin, I. & Denizli, A. Biomedical Applications of Polymeric Cryogels. *Appl. Sci.* **9**, 553 (2019).
34. Mikhalovsky, S. V., Savina, I. N., Dainiak, M., Ivanov, A. E. & Galaev, I. Y. 5.03 - Biomaterials/Cryogels, in Comprehensive *Biotechnology, Second Edition* 11-22 (vol. 5, Academic Press, 2011).
35. Fan, J. A. et al. Fractal design concepts for stretchable electronics. *Nat. Commun.* **5**, 3266 (2014).

36. Liu, Y. et al. High-Performance Flexible All-Solid-State Supercapacitor from Large Free-Standing Graphene-PEDOT/PSS Films. *Sci. Rep.* **5**, 17045 (2015).
37. Zhang, H., Xia, H. & Zhao, Y. Poly(vinyl alcohol) Hydrogel Can Autonomously Self-Heal. *ACS Macro Lett.* **1**, 1233–1236 (2012).
38. Kamoun, E. A., Kenawy, E.-R. S. & Chen, X. A review on polymeric hydrogel membranes for wound dressing applications: PVA-based hydrogel dressings. *J. Adv. Res.* **8**, 217–233 (2017).
39. Xu, X. et al. Effects of Potassium Levels on Plant Growth, Accumulation and Distribution of Carbon, and Nitrate Metabolism in Apple Dwarf Rootstock Seedlings. *Front. Plant Sci.* **11**, 904 (2020).
40. Zakharin, A. A. *Rapid Water Inflow Outflow Plants Roots. Treat. Salt Solut. Var. Concentrations* **48**, 6 (2001).
41. Håkansson, A. et al. Effect of (3-glycidyloxypropyl)trimethoxysilane (GOPS) on the electrical properties of PEDOT:PSS films. *J. Polym. Sci. Part B Polym. Phys.* **55**, 814–820 (2017).
42. Bihar, E. et al. Fully Inkjet-Printed, Ultrathin and Conformable Organic Photovoltaics as Power Source Based on Cross-Linked PEDOT: PSS Electrodes. *Adv. Mater. Technol.* **5**, 2000226 (2020).
43. Bihar, E. et al. Data for Self-healable Stretchable Printed Electronic Cryogels for in-vivo Plant Monitoring, Open Science Framework, https://osf.io/8gzpn/, https://doi.org/10.17605/OSF.IO/8GZPN (2023).

ACKNOWLEDGEMENTS

The authors would like to acknowledge Aseem Visal for his help with the viscosity measurements. This work was supported by the National Science Foundation (NSF) Signals in the Soils (SitS) program (Award No. 1935594), as well as an award from the Natural Environment Research Council (NERC) (reference NE/T012293/1). Microscopic analyses were performed at MIMIC, University of Colorado Boulder (RRID:SCR 019307).

AUTHOR CONTRIBUTIONS

G.L.W. and E.B. conceived and coordinated the research. E.B. designed and performed the experiments with contributions from E.J.S., C.A.C., M.N.R., and M.A. E.B. and T.T. fabricated the device. E.B., G.L.W., and R.R.M. analyzed the data. A.G. performed X-ray computed microtomography images of the stems. M.N.R. helped with the acquisition system. I.B. and E.B. performed histology of the stems. E.J.S., C.A.C., M.N.R. contributed equally. E.B., I.B., C.A.C., and E.J.S. wrote the manuscript. All authors revised the manuscript.

COMPETING INTERESTS

The University of Colorado-Boulder and the authors E.B., E.J.S., and G.L.W. have filed a patent application related to electronic cryogels. The remaining authors declare no competing interests.

ADDITIONAL INFORMATION

Supplementary information The online version contains supplementary material available at https://doi.org/10.1038/s41528-023-00280-1.

Correspondence and requests for materials should be addressed to Eloïse Bihar or Gregory L. Whiting.

Reprints and permission information is available at http://www.nature.com/reprints

Publisher's note Springer Nature remains neutral with regard to jurisdictional claims in published maps and institutional affiliations.